Journal of Thermophysics and Heat Transfer
Vol. 25, No. 3, July–September 2011

Multi-Objective Optimization of Plain Fin-and-Tube Heat Exchanger Using Evolutionary Algorithm

Hassan Hajabdollahi*
ValiAsr University of Rafsanjan, Rafsanjan, Iran
and
Pouria Ahmadi† and Ibrahim Dincer
University of Ontario Institute of Technology, Oshawa, Ontario L1H 7K4, Canada

DOI: 10.2514/1.49976

In the present study, a comprehensive thermal modeling and optimal design of a plain fin-and-tube heat exchanger is performed. Hence, the ε-NTU method is applied to estimate the heat exchanger pressure drop and effectiveness. Some design parameters of this study are selected as follows: longitudinal pitch, transversal pitch, fin pitch, number of tube pass, tube diameter, cold-stream flow length, no-flow length, and hot-stream flow length. In addition, a fast and selective nondominated sorting genetic algorithm (NSGA-II) is applied to obtain the maximum effectiveness and the minimum total annual cost (as a sum of investment and operation costs) as two objective functions. The results of optimal designs are presented in a set of multiple optimum solutions, called Pareto-optimal solutions. Furthermore, a sensitivity analysis of change in optimum effectiveness and total annual cost with changes in design parameters of the fin-and-tube heat exchanger is also performed in detail.

Nomenclature

A	=	heat transfer surface area, m^2
A_{flow}	=	minimum free-flow area on the tube outside, m^2
A_{front}	=	frontal area, m^2
C_c	=	cold flow stream heat capacity rate, W/K
C_h	=	hot flow stream heat capacity rate, W/K
C_{inv}	=	annual cost of investment, /year
$C_{\max}$	=	maximum of C_h and C_c, W/K
$C_{\min}$	=	minimum of C_h and C_c, W/K
C_{ope}	=	annual cost of operation, /year
C_{tot}	=	total annual cost, /year
C^*	=	heat capacity rate ratio, $C_{\min}/C_{\max}$
D_h	=	hydraulic diameter, m
d_c	=	fin collar outside diameter, m
d_i	=	tube inside diameter, m
d_o	=	tube outside diameter, m
f	=	friction factor
G	=	mass flux, kg/m^2 s
h	=	heat transfer coefficient, W/m^2 K
j	=	Culburn number
k_{el}	=	price of electrical energy, MWh^{-1}
L_1	=	cold-stream flow length, m
L_2	=	hot-stream flow length, m
L_3	=	no-flow length, m
NP	=	number of tube passes
NTU	=	number of transfer units
Nu	=	Nusselt number
N_l	=	number of plate in L_1 direction
N_r	=	number of tube row
N_t	=	total number of tube
n	=	exponent of nonlinear increase with area increase
Pr	=	Prandtl number
p_f	=	fin pitch, m
Re	=	Reynolds number
r	=	interest rate
St	=	Stanton number
U	=	overall heat transfer coefficient, W/m^2 K
V	=	heat exchanger volume, m^3
V_t	=	volumetric flow rate, m^3/s
X_l	=	longitudinal pitch, m
X_t	=	transversal pitch, m
y	=	depreciation time, year
ΔP	=	pressure drop, Pa
δ	=	fin thickness, m
ε	=	thermal effectiveness
η_s	=	overall surface efficiency
η_f	=	fin efficiency
η	=	compressor efficiency
λ	=	nondimensional conduction parameter
μ	=	viscosity, Pa $\cdot$ s
ν	=	specific volume, m^3/kg
σ	=	ratio between A_{flow} and A_{front}, $A_{\mathrm{flow}}/A_{\mathrm{front}}$
τ	=	hours of operation per year

Subscripts

ave	=	average
c	=	cold
f	=	fin
h	=	hot
i	=	inside
in	=	inlet
o	=	outside
out	=	outlet
tot	=	total

Introduction

COMPACT heat exchangers are characterized by a large heat transfer surface area per unit volume of the exchanger. A fin-and-tube heat exchanger (FTHE), as shown in Fig. 1, is a typical compact heat exchanger that is widely used in many industrial power-generation plants, chemical, petrochemical, and petroleum industries. Fins or extended surface elements are introduced to increase the heat transfer area [1]. Some of commonly used fins are, wavy, offset strip, louver, perforated, and plain fins [2]. Sanaye and Hajabdollahi [3–5] applied the nondominated sorting genetic algorithm (NSGA-II) and optimized the rotary regenerator, plate fin, and shell-and-tube heat exchangers. Haseli et al. [6] obtained

Received 21 March 2010; revision received 1 January 2011; accepted for publication 4 January 2011. Copyright © 2011 by the American Institute of Aeronautics and Astronautics, Inc. All rights reserved. Copies of this paper may be made for personal or internal use, on condition that the copier pay the $10.00 per-copy fee to the Copyright Clearance Center, Inc., 222 Rosewood Drive, Danvers, MA 01923; include the code 0887-8722/11 and $10.00 in correspondence with the CCC.

*Mechanical Engineering Department.
†Department of Mechanical Engineering, Faculty of Engineering and Applied Science, 2000 Simcoe Street North; Pouria.ahmadi@uoit.ca.

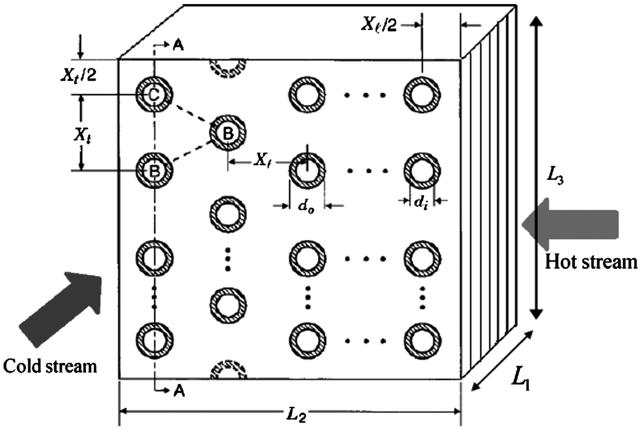

Fig. 1 Typical plain fin-and-tube heat exchanger with staggered-tube arrangement.

optimum cooling-water temperature during condensation of saturated water vapor within a shell-and-tube condenser. Hilbert et al. [7] also used a multi-objective optimization technique to maximize the heat transfer rate and to minimize the pressure drop in a tube-bank heat exchanger. Xie et al. [8] minimized the total volume and the total annual cost of a compact heat exchanger by considering three shape parameters as decision variables. Wang et al. [9] applied genetic algorithm to optimize primary energy saving, annual total cost saving, and carbon dioxide emission reduction. Guo et al. [10] employed genetic algorithm to optimize the field synergy number, which is defined as the indicator of the synergy between the velocity field and the heat flow. Sahin et al. [11] optimized the design parameters of a heat exchanger with rectangular fins by the Taguchi experimental-design method. Doodman et al. [12] minimized the total annual cost of air-cooled heat exchangers using global sensitivity analysis. Foli et al. [13] estimated the optimum geometric parameters of micro-channels in micro heat exchangers by maximizing the heat transfer rate and minimizing the pressure drop as two objective functions. Liu and Cheng [14] optimized a recuperator for the maximum heat transfer effectiveness and minimum exchanger weight and pressure loss. Gholap and Khan [15] also studied air-cooled heat exchangers by minimizing the energy consumption of fans and material cost as two objective functions.

In this paper, it is aimed to first conduct a thermal modeling of a FTHE and later optimize this equipment by maximizing the effectiveness and minimizing the total annual cost. Genetic-algorithm optimization technique is applied to provide a set of the Pareto multiple optimum solutions. The sensitivity analysis of change in optimum values of effectiveness and total annual cost with change in design parameters was performed and the results are reported. In summary, the following are the specific objectives of this paper to the area:

1) The first objective is to thermally model a plain-type fin-and-tube heat exchanger by proposing a closed-form equation to predict the heat transfer coefficient and total annual cost.

2) The second objective is to apply multi-objective optimization for a fin-and-tube heat exchanger, with effectiveness and total annual cost as the two objectives (not considered previously in the given references), using a genetic algorithm.

3) The third objective is to select the longitudinal pitch, transversal pitch, fin pitch, number of tube passes, tube diameter, cold-stream flow length, no-flow length, and hot-stream flow length as design parameters (decision variables).

4) The fourth objective is to propose a closed-form equation for the total annual cost in terms of effectiveness at the optimal design point.

5) The fifth objective is to perform sensitivity analysis of the change in objective functions when the optimum design parameters vary and to find the degree of each parameter on objective functions that are conflicting.

Thermal Modeling

The ε-NTU method is applied here for predicting the heat exchanger performance. The effectiveness of crossflow heat exchanger with both fluids unmixed is proposed as [16] follows:

$$\varepsilon = 1 - \exp[-(1 + C^*)\mathrm{NTU}] \times \Bigg[I_0(2\mathrm{NTU}\sqrt{C^*}) + \sqrt{C^*} I_1(2\mathrm{NTU}\sqrt{C^*}) - \frac{1 - C^*}{C^*} \sum_{n=2}^{\infty} C^{*n/2} I_n(2\mathrm{NTU}\sqrt{C^*}) \Bigg] \tag{1}$$

where I is the modified Bessel function, and number of transfer units (NTU) and heat capacity ratio C^* are defined as follows [1]:

$$\mathrm{NTU}_{\max} = \frac{U_o A_{\mathrm{tot},h}}{C_{\min}} \tag{2}$$

$$C^* = C_{\min}/C_{\max} \tag{3}$$

Here, U_o is the overall heat transfer coefficient for the fin side, defined as follows:

$$U_o = 1 \Bigg/ \left(\frac{1}{h_h \eta_{s,h}} + \frac{1}{(A_{i,c}/A_{\mathrm{tot},h})(h_c \eta_{s,c})} \right) \tag{4}$$

with negligible fouling and wall-conduction resistances. Here, $A_{i,c}$ is the total heat transfer area inside of tube and $A_{\mathrm{tot},h}$ is outside the total heat transfer surface area, including fins and tubes, as follows:

$$A_{\mathrm{tot},h} = A_f + A_{o,c} \tag{5}$$

where A_f and $A_{o,c}$ are the heat transfer surface area of fins and tube outside, respectively, as follows [17]:

$$A_f = 2L_1/p_f(L_2 \times L_3 - N_t \times \pi d_o^2/4) \tag{6}$$

$$A_{o,c} = \pi d_o N_t L_1 - N_t \times \pi d_o \delta(N_1 - 1) \tag{7}$$

where N_t and N_l are the total tube number and the number of plate in the L_1 direction; h is the heat transfer coefficient; δ is the fin thickness; L_1, L_2, and L_3 are cold-stream flow length, hot-stream flow length, and no-flow length, respectively (Fig. 1); η_s in Eq. (4) is the overall surface efficiency defined as follows [1]:

$$\eta_s = 1 - \frac{A_f}{A_{\mathrm{tot},h}}(1 - \eta_f) \tag{8}$$

where η_f is efficiency of a single fin.

The Fanning factor f and Colburn factor j (respectively, representative of pressure drop and of its thermal performances) are defined in Eqs. (9) and (10) by Wang et al. [18] for plain flat fins on a staggered-tube banks as follows:

$$j = \begin{cases} 0.108 Re_{dc}^{-0.29} (X_t/X_l)^{c_1} (p_f/d_c)^{-1.084} (p_f/D_h)^{-0.786} (p_f/X_t)^{c_2} & \text{for } N_r = 1 \\ 0.086 Re_{dc}^{c_3} . N_r^{c_4} (p_f/d_c)^{c_5} (p_f/D_h)^{c_6} (p_f/X_t)^{-0.93} & \text{for } N_r \geq 2 \end{cases} \tag{9}$$

$$f = 0.0267 Re_{dc}^{c_7} (X_t/X_l)^{c_8} (p_f/d_c)^{c_9} \tag{10}$$

where

$$c_1 = 1.9 - 0.23 \ln Re_{dc} \tag{11a}$$

$$c_2 = -0.236 + \ln Re_{dc} \quad (11b)$$

$$c_3 = -0.361 - \frac{0.042N_r}{\ln Re_{dc}} + 0.158 \ln[N_r(p_f/d_c)^{0.41}] \quad (11c)$$

$$c_4 = -1.224 - \frac{0.076(X_l/D_h)^{1.42}}{\ln Re_{dc}} \quad (11d)$$

$$c_5 = -0.083 + \frac{0.058N_r}{\ln Re_{dc}} \quad (11e)$$

$$c_6 = -5.735 + 1.21 \ln \frac{Re_{dc}}{N_r} \quad (11f)$$

$$c_7 = -0.764 + 0.739(X_t/X_l) + 0.177(p_f/d_c) - 0.00758/N_r \quad (11g)$$

$$c_8 = -15.689 + 64.021/ \ln Re_{dc} \quad (11h)$$

$$c_9 = 1.696 - 15.695/ \ln Re_{dc} \quad (11i)$$

The above equations are valid for $300 < Re < 20,000$ and for $6.9 \le d_c \le 13.6$ mm, $1.3 \le D_h \le 9.37$ mm, $20.4 \le X_t \le 31.8$ mm, $12.7 \le X_l \le 32$ mm, $1.0 \le p_f \le 8.7$ mm, and $1 \le N_r \le 6$. The proposed correlations for Colburn number and f factor are accurate within $\pm 15\%$ [18].

The Reynolds number and hydraulic diameter are defined as follows [18]:

$$Re_{dc} = \frac{Gd_c}{\mu} \quad (12)$$

where

$$d_c = d_o + 2\delta \quad (13)$$

and G is mass flux.

The heat transfer coefficient is defined as follows [1]:

$$h = StGc_p \quad (14)$$

where St is given as

$$St = \frac{j}{Pr^{2/3}} \quad (15)$$

where A_{flow} minimum free-flow area on the tube outside, which is given by [17]

$$A_{\text{flow}} = \left[\left(\frac{L_3}{X_t} - 1\right)b + (X_t - d_o)\right]L_1 \quad (17)$$

Here, b is the minimum of $X_t - d_o$ and $2\sqrt{(X_t/2)^2 + X_l^2}$. Furthermore, σ is the ratio of minimum free-flow area to frontal area, and f is the friction factor obtained from Eq. (10).

The Nusselt number and friction coefficient in the tube side are estimated as follows [17]:

$$Nu = \frac{(f/2)(Re - 1000)Pr}{1 + 12.7(f/2)^{1/2}(Pr^{2/3} - 1)} \quad (18)$$

$$f = (1.58 \ln Re - 3.28)^{-2} \quad (19)$$

Influence of Longitudinal Heat Conduction

To evaluate the influence of heat conduction in the flow direction (either in the solid wall or in the fluid), the following approximation for longitudinal conduction analysis is considered. Fluids generally have low thermal conductivities (except for liquid metal), but the wall conductivity may be quite high. Therefore, only wall-conduction effects are considered here. The influence of longitudinal conduction is to reduce exchanger effectiveness for a given number of transfer units, and this reduction may be quiet serious in exchangers with short flow lengths design for high effectiveness values ($\varepsilon > 90\%$) [1]. Assuming the temperature difference δT for the hot fluid is of the same magnitude for the cold fluid ($C_{\min}/C_{\max} \approx 1$) and for the wall, then the wall temperature gradient is $\delta T/L$, with L being the flow length and the longitudinal heat transfer by conduction of the order of that given in Eq. (1). If the wall cross-sectional area for longitudinal conduction is designated as A_k, then

$$q_{\text{cond}} \approx k_w A_k \frac{\delta T}{L} \quad (20)$$

where A_k is the wall cross-sectional area for longitudinal conduction and k_w is the wall-conduction coefficient.

The convection heat transfer rate is also given by energy-balance considerations as follows:

$$q_{\text{conv}} = C_c \delta T = C_h \delta T \quad (21)$$

and then,

$$\frac{q_{\text{cond}}}{q_{\text{conv}}} = \frac{(k_w/L)A_k}{C} = \frac{(k_w/L)A_{\text{fr}}(1-\sigma)}{C_{\min}} = \lambda \quad (22)$$

where λ in Eq. (22) is the nondimensional conduction parameter. The values of λ are computed for various optimal design points as presented in the case study.

Genetic Algorithm for Multi-Objective Optimization

Multi-Objective Optimization

A multi-objective problem consists of optimizing (i.e., minimizing or maximizing) several objectives simultaneously, with a number of inequality or equality constraints. A genetic algorithm (GA) is a semistochastic method, based on an analogy with Darwin's laws of natural selection [19]. The first multi-objective GA, called vector-evaluated GA (or VEGA), was proposed by Schaffer [20]. an algorithm based on nondominated sorting was proposed by Srinivas and Deb [21] and called nondominated sorting genetic algorithm (NSGA). This was later modified by Deb et al. [22], which eliminated higher computational complexity, lack of elitism, and the need for specifying the sharing parameter. This algorithm is called NSGA-II, which is coupled with the objective functions developed in this study for optimization.

Tournament Selection

Each individual competes in exactly two tournaments with randomly selected individuals, a procedure that imitates survival of the fittest in nature.

Controlled Elitism Sort

To preserve diversity, the influence of elitism is controlled by choosing the number of individuals from each subpopulation according to the geometric distribution [23],

$$S_q = S\frac{1-c}{1-c^w}c^{q-1} \quad (23)$$

to form a parent search population, P_{t+1} (t denotes the generation), of size S, where $0 < c < 1$, and w is the total number of ranked nondominated.

Crowding Distance

The crowding distance metric proposed by Deb [24] is used, where the crowding distance of an individual is the perimeter of the rectangle with its nearest neighbors at diagonally opposite corners. So if individual $X^{(a)}$ and individual $X^{(b)}$ have same rank, each one has a larger crowding distance is better.

Crossover and Mutation

Uniform crossover and random uniform mutation are employed to obtain the offspring population, Q_{t+1}. The integer-based uniform crossover operator takes two distinct parent individuals and interchanges each corresponding binary bits with a probability, $0 < p_c \leq 1$. Following crossover, the mutation operator changes each of the binary bits with a mutation probability, $0 < p_m < 0.5$.

Objective Functions, Design Parameters, and Constraints

In this study, effectiveness and total annual cost are considered as two objective functions. Total annual cost is includes investment cost (the annualized cost of the heat transfer surface area) and operating cost of compressor (or pump) to flow the fluid as follows [8]:

$$C_{\text{tot}} = aC_{\text{inv}} + C_{\text{ope}} \tag{24}$$

$$C_{\text{inv}} = C_A \times A_{\text{tot}}^n \tag{25}$$

$$C_{\text{ope}} = \left(k_{\text{el}}\tau \frac{\Delta p V_t}{\eta}\right)_c + \left(k_{\text{el}}\tau \frac{\Delta p V_t}{\eta}\right)_h \tag{26}$$

Here, C_A and k_{el} are the heat exchanger investment cost per unit surface area and the electricity unit cost, respectively; n is a constant; τ is the operation hours of the exchanger per year; Δp, V_t, and η are pressure drop, volume flow rate, and compressor efficiency, respectively; and a is the annual cost coefficient, defined as follows:

$$a = \frac{r}{1 - (1 + r)^{-y}} \tag{27}$$

where r and y are interest rate and depreciation time, respectively. In this study, longitudinal pitch X_l, transversal pitch X_t, fin pitch p_f, number of tube pass NP, outside tube diameter d_o, cold-stream flow length L_1, no-flow length L_3, and hot-stream flow length L_2 were considered as eight design parameters. The constraints are introduced to ensure that d_c, D_h, X_t, X_l, p_f, and N_r are in the range of $6.9 \leq d_c \leq 13.6$ mm, $1.3 \leq D_h \leq 9.37$ mm, $20.4 \leq X_t \leq 31.8$ mm, $12.7 \leq X_l \leq 32$ mm, $1.0 \leq p_f \leq 8.7$ mm, and $2 \leq N_r \leq 6$.

Case Study

In this section, a case study is presented to show how to use the present model. Outlet gases from the compressor with mass flow rate of 2.5 kg/s and temperature of 425 K enters the fin-and-tube precooler heat exchanger. On the other hand, water with a mass flow rate of 3.2 kg/s and temperature of 285 K flow in the other side. The FTHE metal is made of stainless steel with thermal conductivity about $k_w = 25$ W/m · K. The ratio of inside-to-outside tube diameter is taken to be 0.8. The operating conditions and the cost function constants are listed in Table 1. The thermophysical properties of air, such as Prandtl number, kinematic viscosity, and specific heat are considered to be temperature-dependent.

Table 1 Operating conditions of the FTHE (input data for the model)

Mass flow rate of hot flow, kg/s	2.5
Mass flow rate of cold flow, kg/s	3.2
Inlet hot temperature, K	425
Inlet cold temperature, K	285
Inlet pressure (hot side), kPa	250
Inlet pressure (cold side), kPa	200
Price per unit area /m^2	85
Exponent of nonlinear increase with area increase	0.6
Hours of operation per year h/year	5000
Price of electrical energy /MWh	25
Compressor or pump efficiency	0.65

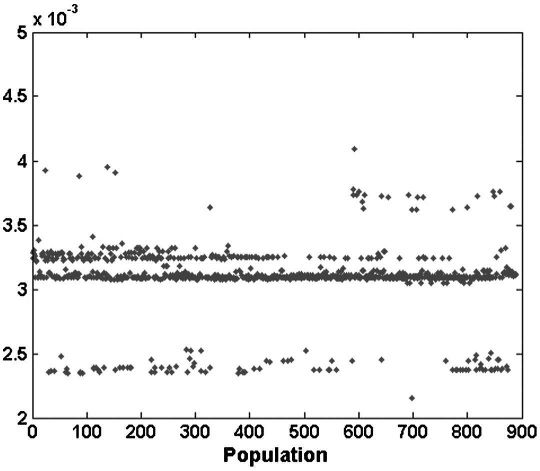

Fig. 2 Distribution of numerical values of λ (the nondimensional heat conduction parameter) in the whole optimal output domain.

Results and Discussion

Longitudinal Heat Conduction

To quantify the effect of longitudinal heat conduction in comparison with the convection heat transfer, the numerical values of λ [Eq. (22)] are computed for $k_w = 25$ W/m · K for all optimum design cases as is shown in Fig. 2. It is then found that the distribution of λ value in the whole optimal output domain shows the numerical values to be less than 0.005 (0.5%). This shows that assuming the negligible conduction heat transfer in our analysis in flow direction is acceptable for the studied problem.

Verification of Modeling and Optimization Results

To verify the modeling results, the simulation output were compared with the corresponding reported results given in [1]. The comparison of our modeling results and the corresponding values from [1] (page 270), for the same input values listed in Table 2, are given in Table 3. The results show that the difference percentage points of two mentioned modeling output results are acceptable.

Optimization Results

To maximize the effectiveness value and to minimize the total annual cost, eight design parameters were selected, including longitudinal pitch, transversal pitch, fin pitch, number of tube pass, tube diameter, cold-stream flow length, no-flow length, and hot-stream flow length. Design parameters (decision variables) and the range of their variations are listed in Table 4. The number of iterations for finding the global extremum in the whole searching domain was about 10^{25}. The system was optimized for depreciation time ($y = 12$ years) and interest rate ($r = 0.12$). The genetic-algorithm optimization was performed for 250 generations, using a search population size of $M = 100$ individuals, crossover probability of $p_c = 0.9$, gene mutation probability of $p_c = 0.035$, and controlled elitism value $c = 0.55$. The results for Pareto-optimal curve are shown in Fig. 3, which clearly reveal the conflict between two objectives, the effectiveness, and the total annual cost. Any geometrical change that increases the effectiveness or heat transfer

Table 2 Geometrical characteristic of plain fin-and-tube heat exchanger from [1]

Variables	Value
Longitudinal pitch, mm	22
Transversal pitch, mm	25.4
Fin pitch, mm	3.175
Outside tube diameter, mm	10.2
Fin thickness, mm	0.33
Reynolds number	1968

Table 3 Comparison of modeling output and the corresponding results from [1]

Output variables	Ref. [1]	Present paper	Difference, %
D_h, mm	3.632	3.368	−7.26
A_{flow}/A_{front}	0.534	0.495	−7.3
A_{tot}/V (m^2/m^3)	587	587.76	0.13
A_h/A_{tot}	0.913	0.915	0.35
j	0.008	0.0091	13.75
f	0.0263	0.0299	13.68

Table 4 Design parameters, their range of variation and their change step

Variables	From	To	Change step
Longitudinal pitch, mm	12.7	32	1
Transversal pitch, mm	20.4	31.8	1
Fin pitch, mm	1	8.7	1
Number of tube pass, -	2	6	2
Outside tube diameter, mm	7	10	1
Cold-stream flow length, m	0.2	1	0.001
No-flow length, m	0.2	1	0.001
Hot-stream flow length, m	0.05	0.2	0.001

rate ($\varepsilon = q/q_{max}$) leads to an increase in the total annual cost and vice versa. This shows the need for multi-objective optimization techniques in optimal design of a FTHE. It is shown in Fig. 3 that the maximum effectiveness exists at design point A (0.9406), whereas the total annual cost is the biggest at this point. On the other hand, the minimum total annual cost occurs at design point E ($195.1), with the smallest effectiveness value (0.1885) at that point. Design point A is the optimal situation at which effectiveness is a single objective function, and design point E is the optimum condition at which total annual cost is a single objective function.

The optimum values of two objectives for five typical points from A to E (Pareto-optimal fronts) for input values given in Table 1 are listed in Table 5.

To provide a useful tool for the optimal design of the FTHE, the following equation for effectiveness versus the total annual cost was derived for the Pareto curve (Fig. 3):

$$C_{total}() = \frac{-586.3\varepsilon^2+33.45\varepsilon+536.3}{\varepsilon^2-323.6\varepsilon+3075} \times 1000 \tag{28}$$

which is valid in the range of $0.1885 < \varepsilon < 0.9406$ for effectiveness. The interesting point is that considering a numerical value for the effectiveness in mentioned range provides the minimum total annual cost for that optimal point, along with other optimal design parameters.

The selection of the final solution among the optimum points existing on the Pareto front needs a process of decision-making. In

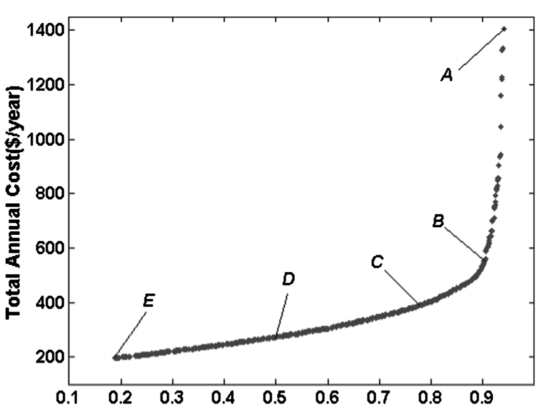

Fig. 3 Distribution of Pareto-optimal points solutions using NSGA-II.

Table 5 Optimum values of effectiveness and the total annual cost for the design points A to E in Pareto-optimal fronts for input values given in Table 1

	A	B	C	D	E
Effectiveness	0.9406	0.9044	0.7795	0.5	0.1885
Total annual cost, $	1404	552.5	389.4	273.4	195.1

fact, this process is mostly carried out based on engineering experiences and the importance of each objective for decision-makers. In this paper, based on information provided for designers (the practical effectiveness values in the range of $0.5 < \varepsilon < 0.78$), the design points (C–D) with reasonable total cost and effectiveness values are recommended.

The distribution of variables for the optimal points on the Pareto front (Fig. 3) is shown in Figs. 4a–4h. The lower and upper bounds of the variables are shown by dotted lines. The following points for the optimal variables in Fig. 4 could be deduced:

1) The longitudinal pitch, transversal pitch, fin pitch, no-flow length, and hot-stream flow length have the values relatively distributed in its allowable domain.

2) The numerical values of the cold-stream flow length, number of tube passes, and tube diameter are at their maximum level.

Since the optimum values of five decision variables have scattered distribution in their allowable domains, one may predict that these five parameters have important effects on the conflict between the higher values of effectiveness and lower amounts of total annual cost. The cold-stream flow length, number of tube passes, and tube diameter (which is situated at its maximum value) show that these parameters have no effect on the conflict between the two objective functions and improve both objective functions at their maximum value. The variation of optimum value of effectiveness with the total annual cost for various values of optimum design parameters in cases A–E (Pareto front) are shown in Figs. 5a–5h. It was observed that the variation of two objective functions at other points on the Pareto-optimal front had the same trend as the five points (A–E). The effect of design variables on objective functions are investigated and explained as follows:

Cold-Stream Flow Length

Based on the information in Fig. 5a, it is found that by increase in the cold-stream flow length heat exchanger effectiveness is increased and annual cost decreases. Therefore, this increment leads to improvement in both objective functions. Thus, the optimal value should be selected. The scattering distribution of optimal points in Fig. 4a confirms this idea.

Hot-Stream Flow Length

As shown in Fig. 5b, increasing the hot-stream flow length results in increase in both effectiveness and total annual cost. Therefore, increase in this parameter in the allowable range leads to conflict between two objective functions. The relative scattering distribution in Fig. 4b confirms this point.

No-Flow Length

The same as hot flow length, by increasing the no-flow length, both effectiveness and annual cost increase simultaneously. As increasing this variable results in the conflict between two objective functions. The relative scattering distribution in Fig. 4c confirms this point.

Fin Pitch

Like hot flow length and no-flow length, by increasing the pitch ratio, both effectiveness and annual cost increase simultaneously in the case that increasing this variable leads to the conflict between two objective functions. The scattering distribution in Fig. 4d confirms this point. As shown in Fig. 5b, increasing this variable in the allowable range has a significant effect on the effectiveness, but it has a negligible effect on the annual cost.

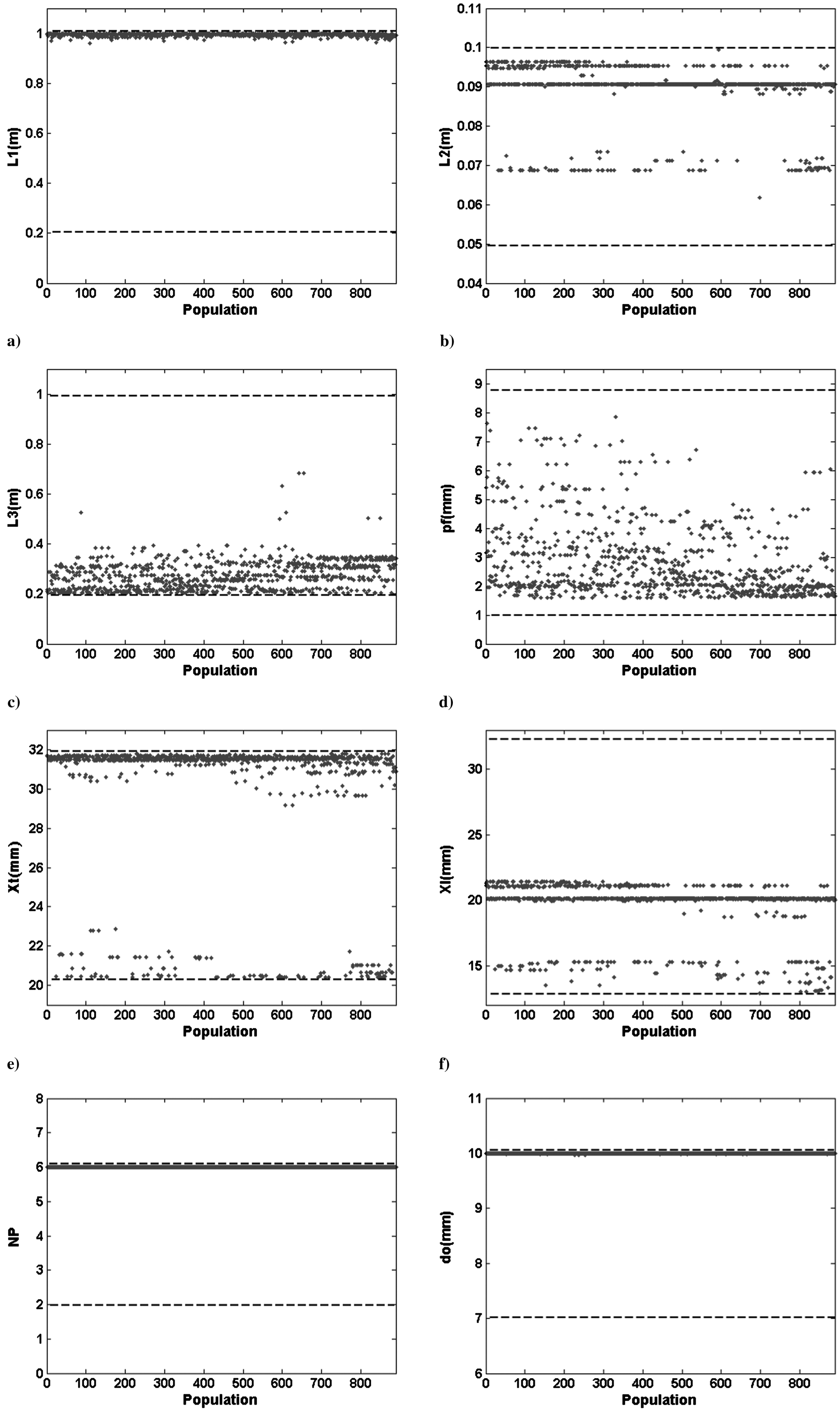

Fig. 4 Scattering of variables for the Pareto-optimal front: a) cold-stream flow length, b) hot-stream flow length, c) no-flow length, d) fin pitch, e) transversal pitch, f) longitudinal pitch, g) number of tube pass, and h) tube diameter.

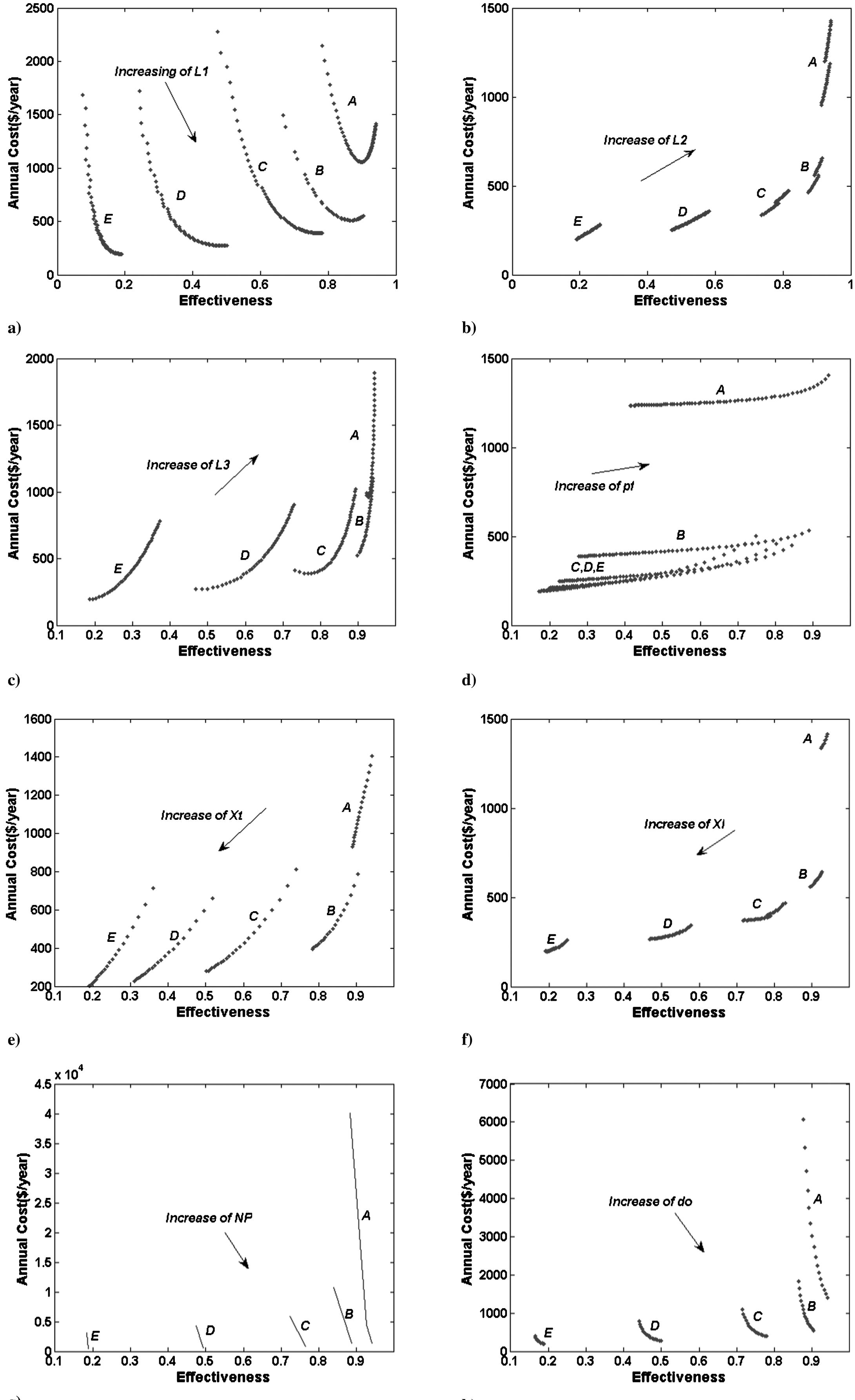

Fig. 5 Variation of effectiveness with annual cost for eight optimum design parameters in five cases of A–E. a) cold-stream flow length, b) hot-stream flow length, c) no-flow length, d_ fin pitch, e_ transversal pitch, f_ Longitudinal pitch, g_ number of tube pass, and h) tube diameter.

Transversal Pitch

According to Fig. 5e, by increasing in the transversal pitch (unlike the other three variables), effectiveness and annual cost decrease simultaneously, as the variation of this variable in the allowable range results in the conflict between two objective functions in the optimal points. The scattering distribution in Fig. 4c confirms this point.

Longitudinal Pitch

The effect of longitudinal pitch is similar to transversal pitch. In this case, by increasing the longitudinal pitch, effectiveness and annual cost decrease simultaneously (Fig. 5f); this trend results in selecting a scattering distribution (Fig. 4f.

Number of Tube Passes

Based on Fig. 5g, by increasing the tube passes, the effectiveness increases, whereas annual cost decreases. Therefore, the optimal value of this variable is suitable for the optimization. Hence, number 6 for the number of tube passes in Fig. 4g shows this point.

Tube Diameter

Like the number of tube passes, by increasing the tube diameter, heat exchanger effectiveness increases, whereas annual cost decreases (Fig. 5h). Selecting the maximum value for the tube diameter in Fig. 4h confirms this point.

Conclusions

In the present paper, a complete thermodynamic modeling of the plain fin heat exchanger has been carried out. For this task, a fin-and-tube heat exchanger is optimally designed using multi-objective optimization technique. The design parameters (decision variables) considered here are longitudinal pitch, transversal pitch, fin pitch, number of tube pass, tube diameter, cold-stream flow length, no-flow length, and hot-stream flow length. In the presented optimization problem, the effectiveness and total annual cost are two objective functions (as the effectiveness is maximized and the total annual cost is minimized). A set of the Pareto-optimal front points are identified. Furthermore, the distribution of each design parameters in their allowable range is shown. The results revealed the level of conflict between these two objectives. Moreover, the correlation between the optimal values of two objective functions is proposed. The longitudinal pitch, transversal pitch, fin pitch, no-flow length, and hot-stream flow length are found to be important design parameters that caused a conflict between effectiveness and the total annual cost. The results show that by increase in the cold-stream flow length, heat exchanger effectiveness increases and annual cost decreases. In addition, increasing the hot-stream flow length results in increase in both effectiveness and total annual cost. Therefore, increase in this parameter in the allowable range leads to conflict between two objective functions. Finally, it is found that each point in the Pareto frontier becomes an optimized point that strongly depends on the decision-maker. However, some points in the Pareto frontier have more advantages in comparison with the rest. A good decision-maker is one who selects the points for which the two objective functions coincide.

References

[1] Kays, W. M., and London, A. L., *Compact Heat Exchangers*, 3rd ed., McGraw–Hill, New York, 1984.

[2] Kim, B., and Sohn, B., "An Experimental Study of Flow Boiling in a Rectangular Channel with Offset Strip Fins," *International Journal of Heat and Fluid Flow*, Vol. 27, 2006, pp. 514–521. doi:10.1016/j.ijheatfluidflow.2005.11.008

[3] Sanaye, S., and Hajabdollahi, H., "Multi-Objective Optimization of Rotary Regenerator Using Genetic Algorithm," *International Journal of Thermal Sciences*, Vol. 48, 2009, pp. 1967–1977. doi:10.1016/j.ijthermalsci.2009.02.008

[4] Sanaye, S., and Hajabdollahi, H., "Thermal-Economic Multi-Objective Optimization of Plate Fin Heat Exchanger Using Genetic Algorithm," *Applied Energy*, Vol. 87, 2010, pp. 1893–1902. doi:10.1016/j.apenergy.2009.11.016

[5] Sanaye, S., and Hajabdollahi, H., "Multi-Objective Optimization of Shell and Tube Heat Exchangers," *Applied Thermal Engineering*, Vol. 30, 2010, pp. 1937–1945. doi:10.1016/j.applthermaleng.2010.04.018

[6] Haseli, Y., Dincer, I., and Naterer, G. F., "Optimum Temperatures in a Shell and Tube Condenser with Respect to Exergy," *International Journal of Heat and Mass Transfer*, Vol. 51, 2008, pp. 2462–2470. doi:10.1016/j.ijheatmasstransfer.2007.08.006

[7] Hilbert, R., Janiga, G., Baron, R., and Thevenin, D., "Multi-Objective Shape Optimization of a Heat Exchanger Using Parallel Genetic Algorithms," *International Journal of Heat and Mass Transfer*, Vol. 49, 2006, pp. 2567–2577. doi:10.1016/j.ijheatmasstransfer.2005.12.015

[8] Xie, G. N., Sunden, B., and Wang, Q. W., "Optimization Of Compact Heat Exchangers by a Genetic Algorithm," *Applied Thermal Engineering*, Vol. 28, 2008, pp. 895–906. doi:10.1016/j.applthermaleng.2007.07.008

[9] Wang, J.-J., Jing, Y.-Y., and Zhang, C. F., "Optimization of Capacity and Operation for CCHP System by Genetic Algorithm," *Applied Energy* (to be published).

[10] Guo, J., Xu, M., and Cheng, L., "The Application of Field Synergy Number in Shell-and-Tube Heat Exchanger Optimization Design," *Applied Energy*, Vol. 86, No. 10, Oct. 2009, pp. 2079–2087. doi:10.1016/j.apenergy.2009.01.013

[11] Sahin, B., Yakut, K., Kotcioglu, I., and Celik, C., "Optimum Design Parameters of a Heat Exchanger," *Applied Energy*, Vol. 82, 2005, pp. 90–106. doi:10.1016/j.apenergy.2004.10.002

[12] Doodman, A. R., Fesanghary, M., and Hosseini, R., "A Robust Stochastic Approach for Design Optimization of Air-Cooled Heat Exchangers," *Applied Energy*, Vol. 86, 2009, pp. 1240–1245. doi:10.1016/j.apenergy.2008.08.021

[13] Foli, K., Okabe, T., Olhofer, M., Jin, Y., and Sendhoff, B., "Optimization of Micro Heat Exchanger: CFD, Analytical Approach and Multi-Objective Evolutionary Algorithms," *International Journal of Heat and Mass Transfer*, Vol. 49, 2006, pp. 1090–1099. doi:10.1016/j.ijheatmasstransfer.2005.08.032

[14] Liu, Z., and Cheng, H., "Multi-Objective Optimization Design Analysis of Primary Surface Recuperator for Microturbines," *Applied Thermal Engineering*, Vol. 28, 2008, pp. 601–610. doi:10.1016/j.applthermaleng.2007.04.010

[15] Gholap, A. K., and Khan, J. A., "Design and Multi-Objective Optimization of Heat Exchangers for Refrigerators," *Applied Energy*, Vol. 84, 2007, pp. 1226–1239. doi:10.1016/j.apenergy.2007.02.014

[16] Franco, A., and Giannini, N., "Optimum Thermal Design of Modular Compact Heat Exchangers Structure for Heat Recovery Steam Generators," *Applied Thermal Engineering*, Vol. 25, 2005, pp. 1293–1313. doi:10.1016/j.applthermaleng.2004.08.018

[17] Shah, R. K., and Sekulic, P., *Fundamentals of Heat Exchanger Design*, Wiley, New York, 2003.

[18] Wang, C. C., Chi, K. U., and Chang, C. J., "Heat Transfer and Friction Characteristics of Plain Fin-and-Tube Heat Exchanger, Part 2: Correlation," *International Journal of Heat and Mass Transfer*, Vol. 43, 2000, pp. 2693–2700. doi:10.1016/S0017-9310(99)00333-6

[19] Goldberg, D. E., *Genetic Algorithms in Search, Optimization and Machine Learning*, Addison-Wesley, Reading, MA, 1989.

[20] Schaffer, J. D., "Multiple Objective Optimization with Vector Evaluated Genetic Algorithms," *Proceedings of the International Conference on Genetic Algorithms and Their Applications*, 1985.

[21] Srinivas, N., and Deb, K., "Multi-Objective Optimization Using Nondominated Sorting in Genetic Algorithms," *Evolutionary Computation*, Vol. 2, No. 3, 1994, pp. 221–48. doi:10.1162/evco

[22] Deb, K., Pratap, A., Agarwal, S., and Meyarivan, T., "A Fast and Elitist Multi-Objective Genetic Algorithm: NSGA-II," *IEEE Transactions on Evolutionary Computation*, Vol. 6, No. 2, 2002, pp. 182–97. doi:10.1109/4235.996017

[23] Deb, K., and Goel, T., "Controlled Elitist Nondominated Sorting Genetic Algorithms for Better Convergence," *Proceedings of the First International Conference on Evolutionary Multi-Criterion Optimization*, Zurich, 2001, pp. 385–99.

[24] Deb, K., *Multi-Objective Optimization Using Evolutionary Algorithms*, Wiley, Chichester, England, U.K., 2001.